Romanian Reports in Physics, Vol. 66, No. 1, P. 99–108, 2014

NUMERICAL SOLUTION OF FOKKER-PLANCK EQUATION FOR ENERGY STRAGGLING OF PROTONS*

HOUSHYAR NOSHAD[1], SEYYEDEH SAMIRA BAHADOR[2]

[1] Amirkabir University of Technology, Tehran Polytechnic, Department of Energy Engineering and Physics, P.O. Box 15875-4413, Hafez Avenue, Tehran, Iran,
E-mail: hnoshad@aut.ac.ir
[2] Payame Noor University, Department of Physics, P.O. Box 19395-3697, Tehran, Iran.
Email: bahador@phd.pnu.ac.ir

Received March 14, 2013

Abstract. Homotopy perturbation method (HPM) was employed to evaluate radial flux distribution for a pencil beam of 60 MeV protons passing thorough muscle and bone tissues. Afterwards, trajectories of 60 MeV protons and their depth dose distributions in the tissues were determined. Moreover, lateral broadening of dose delivered to the tissues by 60 MeV protons was computed at different depths. The high accuracy of HPM was benchmarked *via* comparison of our results with those obtained from the high charge and energy transport (HZETRN) model, Monte Carlo simulation, GEANT4.5.2 computer code and the experimental data reported in the literature.

Key words: homotopy perturbation method, trajectory of protons, depth dose distribution; lateral broadening of dose, hadrontherapy.

1. INTRODUCTION

Hadrontherapy is a powerful technique in radiation therapy which employs ion beams specially, protons and carbon ions for treatment of deep-seated tumors [1, 2]. Notably, Clinical trials using these beams are now in progress. For instance, up to July 2010, several clinical heavy ion therapy facilities have been working worldwide [3]. The advantages of ion beams in cancer treatment with respect to conventional radiotherapy are their characteristic Bragg peak, small lateral spreading as well as increased relative radiobiological effectiveness (RBE). Remarkably, protons are mostly used in clinical practice due to several hospital-based centers in operation worldwide [4]. For example, by the end of 2009, about 77,300 patients worldwide have been treated with proton and 7,100 with carbon

* Paper presented at the 1st Annual Conference of the Romanian Society of Hadrontherapy (ICRSH 2013), February 21–24, 2013, Predeal, Romania.

radiotherapy [5]. The extended use of proton beams in clinical radiotherapy and afterwards fundamental rule of dose in proton therapy have resulted in investigation on depth dose distribution of this beam in a medium. Furthermore, since the conformity of dose broadening with tumor volume has been emphasized in radiation therapy, radial broadening of the absorbed dose in the Bragg peak should be precisely estimated as well.

For dose calculation in proton therapy, some techniques such as pencil-beam method [6–8] and Monte Carlo (MC) simulation have been proposed in the literature. Even though pencil-beam method is widely employed for proton therapy, its accuracy is significantly reduced in heterogeneous media [9]. Moreover, MC simulation has been regarded as the most accurate method for dose calculation in radiotherapy. It is worthwhile to note that the high precision in this method can be obtained by a large number of particles simulated. As this process takes a long time, some new techniques have been proposed to accelerate the MC dose calculation process [10–12]. An alternative for proton dose calculation is to solve a stochastic differential equation namely, Boltzmann transport equation. Assuming small angle Coulomb interactions in Boltzmann equation gives a Fokker-Planck equation (FPE) [13]. FPE is a stochastic differential equation which characterizes the distribution of heavy charged particles in a medium. Several approximate techniques are reported in the literature for solving the FPEs [14–18].

Homotopy Perturbation Method (HPM) is combination of perturbation and homotopy methods which is useful for obtaining a closed form and explicit solution as well as numerical approximations of wide range of linear and nonlinear differential equations [19–23]. Unlike the traditional numerical methods, this technique does not need discretization and linearization. One of the most remarkable features of HPM is that usually just a few perturbation terms are adequate to obtain a reasonably accurate solution. Furthermore, the perturbation equation can be constructed in many ways by homotopy in topology and also the initial approximation can be freely chosen.

In this paper, radial distribution of a pencil beam of 60 MeV protons traversing muscle and bone tissues has been investigated via solving a FPE using HPM. Furthermore, the trajectories of the proton beam inside the tissues have been estimated and compared with the data of High Charge and Energy Transport (HZETRN) model [13]. Besides, depth dose distribution and lateral broadening in absorbed dose have been computed for the protons at various depths of the tissues as well as in the Bragg peak. It is worthwhile to note that the satisfactory agreement was found between our results and those obtained by GEANT4.5.2 code [24] as well as Monte Carlo simulations [25]. Afterwards, for 160.7 Mev protons incident on water, the computed depth dose distribution by HPM compared with experimental data of Paganetti [24] to verify and validate the homotopy technique as well.

2. FOKKER-PLANCK EQUATION

Radial broadening of an ion beam in a medium is due to some random Coulomb interactions with the electrons and nuclei of the target. The FPE is a stochastic differential equation which describes straggling of an ion beam within an absorbing medium. Notably, this equation can be obtained by considering small angle scattering limit in Boltzmann equation [13]. By considering Rutherford scattering of ion-nucleus, the transport of incident protons through a homogenous medium can be characterized *via* following equation [13].

$$\left(\theta_x \frac{\partial}{\partial x} + \theta_y \frac{\partial}{\partial y} + \frac{\partial}{\partial z}\right) \phi(x,y,z,\theta_x,\theta_y) = \frac{1}{\lambda(z)} \left(\frac{\partial^2 \phi}{\partial {\theta_x}^2} + \frac{\partial^2 \phi}{\partial^2 \theta_y}\right), \quad (1)$$

in which $\phi(x,y,z,\theta_x,\theta_y)$ and $\frac{1}{\lambda(z)}$ denote flux distribution of protons and diffusion coefficient, respectively. In addition, θ_x and θ_y are projections of the scattering angle θ on the two perpendicular planes containing the initial beam direction (*i.e.*, the *z* axis) [13]. The diffusion coefficient for protons passing thorough a composite target can be expressed by [26]:

$$\frac{1}{\lambda(z)} = \frac{\pi}{4} \frac{e^4 N_A}{E(z)^2} \sum_i \frac{w_{Ti} Z_{Ti}(Z_{Ti}+1)}{A_{Ti}} \left[\left(1+{\theta_{ri}}^2\right)^{-1} + \ln\left(1+{\theta_{ri}}^2\right) - 1\right]. \quad (2)$$

In Eq. (2) the sum is over the chemical constituents of the target material. Moreover, w_T, Z_T and A_T are weight percent and atomic as well as mass numbers of the target components. Furthermore, $E(z)$ represents the energy of protons at depth *z* in the target and can be computed using the data taken from the stopping and range of ions in matter (SRIM) computer code. Notably, considering the screening of nuclear charge by orbital electrons as well as supposing the finite size for the nucleus in Rutherford scattering cross section restrict the scattering angle of protons as $\theta_1 < \theta < \theta_2$ [26]. In Eq. (2), the quantity θ_r characterizes the ratio of the upper to lower scattering angle.

$$\theta_r = \frac{\theta_2}{\theta_1} = \left[195.36\, Z_T^{-1/3} \left(\frac{Z_T}{A_T}\right)^{1/6}\right]^2. \quad (3)$$

Assuming $\phi(x,y,z,\theta_x,\theta_y) = \phi(z,x,\theta_x)\phi(z,y,\theta_y)$ in Eq. (1) and afterwards applying the separation of variable technique to Eq. (1) yield the Fermi-Eyges equations as follows [27].

$$\frac{\partial\phi(z,x,\theta_x)}{\partial x}+\frac{1}{\theta_x}\frac{\partial\phi(z,x,\theta_x)}{\partial z}=\frac{1}{\theta_x\lambda(z)}\frac{\partial^2\phi(z,x,\theta_x)}{\partial\theta_x{}^2}, \tag{4}$$

$$\frac{\partial\phi(z,y,\theta_y)}{\partial y}+\frac{1}{\theta_y}\frac{\partial\phi(z,y,\theta_y)}{\partial z}=\frac{1}{\theta_y\lambda(z)}\frac{\partial^2\phi(z,y,\theta_y)}{\partial\theta_x{}^2}. \tag{5}$$

In this article, the distribution functions $\phi(z,y,\theta_y)$ and $\phi(z,x,\theta_x)$ have been computed via HPM for a pencil beam of 60 MeV protons incident on muscle as well as bone tissues. The comparison of our results with those reported in the literature support the validity of homotopy perturbation technique.

3. HOMOTOPY PERTURBATION METHOD

The basic concept of HPM is found in the literature [28-30]. Applying this technique to Eq. (4), a homotopy can be constructed as follows:

$$\frac{\partial\phi(z,x,\theta_x)}{\partial x}+p\left(\frac{1}{\theta_x}\frac{\partial\phi(z,x,\theta_x)}{\partial z}\right)-p\left(\frac{1}{\theta_x\lambda(z)}\frac{\partial^2\phi(z,x,\theta_x)}{\partial\theta_x{}^2}\right)=0. \tag{6}$$

The initial condition for Eq. (6) is assumed to have the form

$$\phi(x=0,z,\theta_x)=\frac{1}{4\pi\sqrt{B(z)}}e^{-\frac{A_2(z)\theta_x^2}{4B(z)}}. \tag{7}$$

In Eq. (7), $B(z)=A_0(z)A_2(z)-A_1(z)^2$, where

$$A_0(z)=\int_0^z\frac{d\acute{z}}{\lambda(\acute{z})}d\acute{z},\ A_1(z)=\int_0^z\frac{z-\acute{z}}{\lambda(\acute{z})}d\acute{z},\ A_2(z)=\int_0^z\frac{(z-\acute{z})^2}{\lambda(\acute{z})}d\acute{z}. \tag{8}$$

The functions in Eq. (8) depict integral moments of the diffusion coefficient [13]. In according to homotopy perturbation theory, the solution of Eq. (6) can be regarded in a series of p terms:

$$\phi(z,x,\theta_x)=\phi_0(z,x,\theta_x)+p\phi_1(z,x,\theta_x)+p^2\phi_2(z,x,\theta_x)+\cdots. \tag{9}$$

Inserting Eq. (9) in to Eq. (6) as well as rearranging based on powers of p - terms yield the following perturbation terms

$$p^0:\ \frac{\partial\phi_0(z,x,\theta_x)}{\partial x}=0\rightarrow\phi_0(z,x,\theta_x)=\phi(x=0,z,\theta_x)$$
$$-\frac{1}{4\pi\sqrt{B(z)}}e^{-\frac{A_2(z)\theta_x^2}{4B(z)}},\tag{10}$$

$$p^1:\ \frac{\partial\phi_1(z,x,\theta_x)}{\partial x}+\frac{1}{\theta_x}\frac{\partial\phi_0(z,x,\theta_x)}{\partial z}-\frac{1}{\theta_x\lambda(z)}\frac{\partial^2\phi_0(z,x,\theta_x)}{\partial\theta_x^2}=0$$
$$\rightarrow\phi_1(z,x,\theta_x)=xe^{-\frac{1A_2(z)\theta_x^2}{4\ B(z)}}\left(\frac{1}{8}\frac{\frac{dB(z)}{dz}}{\pi\theta_xB(z)^{\frac{3}{2}}}+\frac{1}{16}\frac{\theta_x\frac{dA_2(z)}{dz}}{\pi B(z)^{\frac{3}{2}}}-\frac{1}{16}\frac{\theta_xA_2(z)\frac{dB(z)}{dz}}{\pi B(z)^{\frac{5}{2}}}\right.\tag{11}$$
$$\left.-\frac{1}{8}\frac{A_2(z)}{\lambda(z)\pi\theta_xB(z)^{\frac{3}{2}}}+\frac{1}{16}\frac{A_2(z)^2\theta_x}{\lambda(z)\pi B(z)^{\frac{5}{2}}}\right),$$
$$p^2:\ \frac{\partial\phi_2(z,x,\theta_x)}{\partial x}+\frac{1}{\theta_x}\frac{\partial\phi_1(z,x,\theta_x)}{\partial z}-\frac{1}{\theta_x\lambda(z)}\frac{\partial^2\phi_1(z,x,\theta_x)}{\partial\theta_x^2}=0$$
$$\rightarrow\phi_2(z,x,\theta_x)=\cdots.$$

Here, the higher order perturbation terms have been omitted because they are too long to be written. According to SRIM computer code, the weight percents of the target constituents have been taken to be H (63.48%), C (6.28%), N (1.57%) and O (28.66%) for muscle and H (53.73%), C (19.58%), O (28.66), P (1.91%) and Ca (3.11%) for bone. In addition, the densities of the muscle as well as bone are considered as 1 g/cm^3 and 1.85 g/cm^3, respectively. Hence, inserting these data in to Eq. (2) gives the diffusion coefficients for 60 MeV protons in the tissues.

$$\begin{cases}\frac{1}{\lambda(z)}=\frac{0.16}{E(z)^2}, & \text{(Mucle tissue)}\\ \frac{1}{\lambda(z)}=\frac{0.056}{E(z)^2}, & \text{(Bone tissue)},\end{cases}\tag{12}$$

where $E(z)$ and $\lambda(z)$ have been characterized in units MeV and mm, respectively. By inserting the diffusion coefficient in to Eqs. (8) and (11) and afterwards by substituting Eqs. (10) and (11) in Eq. (9), having them simplified as well as assuming $p=1$ in Eq. (9), the projected distribution function $\phi(z,x,\theta_x)$ can be ascertained. It is worth noting that as Eqs. (4) and (5) are equivalent, $\phi(z,y,\theta_y)$ can be determined *via* replacing *x* by *y* in Eqs. (7, 9–11) as well. Besides, the radial flux distribution of 60 MeV protons passing through the tissues is extracted from the projected distributions using the integration over θ_x and θ_y as follows:

$$f(x,y,z) = \int_{-\infty}^{+\infty} d\vartheta_x \int_{-\infty}^{+\infty} d\theta_y \, \phi(z,x,\theta_x)\phi(z,y,\theta_y). \tag{13}$$

For example, the radial flux distribution for 60 MeV protons propagating at z = 30 mm depth in muscle tissue can be obtained as:

$$f(x,y,z = 30\,\text{mm}) = \\ = \frac{1}{\pi}[0.634 - 0.255x^2 + 0.051x^4 - 0.056x^6][0.634 - 0.255y^2 \\ + 0.051y^4 - 0.056y^6]. \tag{14}$$

Most noteworthy, the flux distribution in Eq. (14) follows a Gaussian distribution function.

$$f(x,y,z = 30\,\text{mm}) = \frac{0.4}{\pi}\exp\left(\frac{-(x^2+y^2)}{2.5}\right). \tag{15}$$

Correspondingly, the radial flux distribution for 60 MeV protons at different depths of bone tissue can be computed in a similar way.

4. RESULTS AND DISCUSSION

The Fermi-Eyges equations describing straggling of an ion beam in a matter were numerically solved *via* homotopy perturbation method. Afterwards, radial broadening of 60 MeV protons travelling through muscle and bone tissues was evaluated and consequently the trajectories of 60 MeV protons in the tissues have been depicted in Fig. 1.

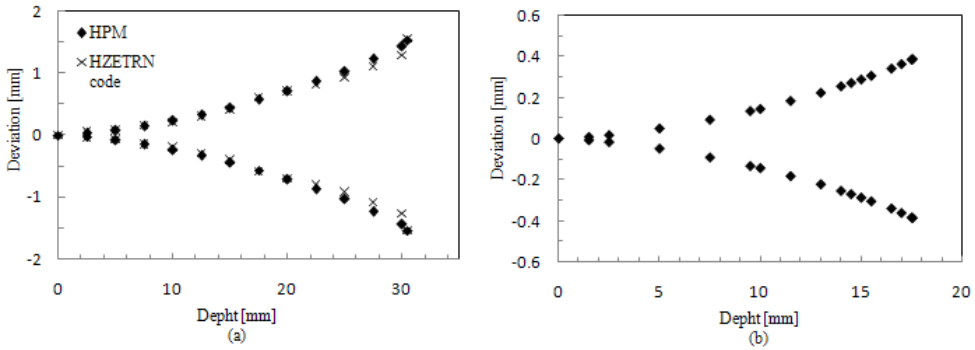

Fig. 1 – Trajectories for a monoenergetic beam of 60 MeV protons in (a) muscle and (b) bone tissues.

Worth fully, in Fig. 1 (a), an excellent overlapping of our results and the data supplied by HZETRN computer code [27] affirms the high accuracy of the HPM. In addition, Fig. 2 illustrates depth dose distributions for the proton beam within the tissues. Most noteworthy, for 60 MeV protons in muscle tissue, the position of Bragg peak determined by HPM is at 30.5 mm depth of the tissue which is consistent with data of GEANT4.5.2 code [24] as well as Monte Carlo simulations [25] within the uncertainties of 2.3% and 0.16%, respectively. Besides, the Bragg peak position of the protons in the bone tissue ($z = 17.5\ mm$) is about 5.12% greater than the results obtained using the GEANT4.5.2 computer code [24].

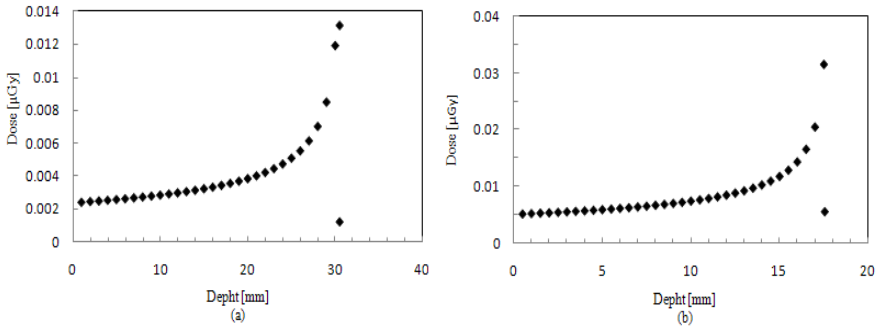

Fig. 2 – Depth dose distribution for a pencil beam of 60 MeV protons passing through: a) muscle; b) bone tissues.

Furthermore, Fig. 3 represents the lateral broadening in relative dose for 60 MeV protons after traversing different depths in the tissues as well as in the Bragg peak. It is worthwhile to note that lateral broadening of dose in Bragg peak provides an appropriate estimate of the size of the tumor located at the end of the path length. For the pencil beam of protons, the Bragg peak is very sharp. Thus in order to irradiate a typical tumor properly, the thickness of the tumor in the beam direction must be very small. Moreover, its thickness in the lateral direction should be equal to the FWHM of lateral distribution in the Bragg peak. According to curve (a), the FWHM in the Bragg peak was obtained to be 2.8 mm. It can be concluded from this analysis that a thin disk-shaped tumor with diameter 3 mm located at 30.55 mm depth of muscle can be irradiated by a pencil beam of 60 MeV protons. Remarkably, in Fig. 4, the computed depth dose distribution using the HPM for 160.7 MeV protons traversing water has been compared with the experimental data of Paganetti [24] to verify and validate the homotopy perturbation technique. The comparison demonstrates that the position of the Bragg peak in our computation is consistent with the data published in the literature [24] with the relative error of 0.57%.

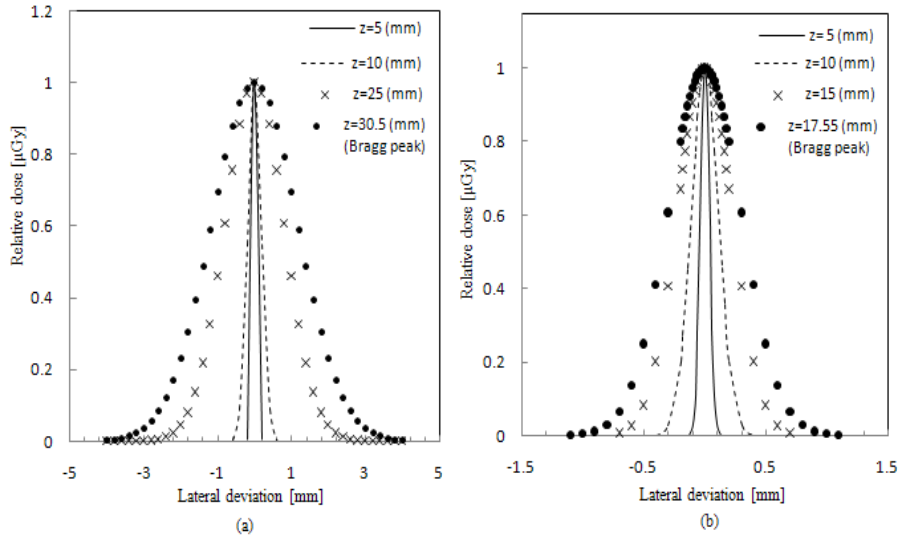

Fig. 3 – Lateral distribution of dose delivered to the (a) muscle as well as (b) bone tissues by a beam of 60 MeV protons at different depths as well as in the Bragg peak.

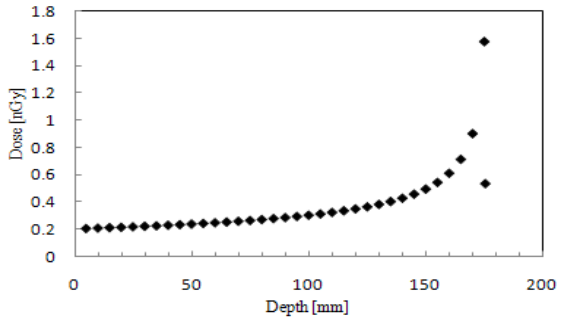

Fig. 4 – Computed depth dose distribution for 160.7 MeV protons in water using HPM.

5. CONCLUSION

In this article, investigations on radial dispersion of a pencil beam of 60 MeV protons passing through muscle and bone tissues were carried out using a numerical technique namely, the homotopy perturbation method. For instance, the lateral broadening of 60 MeV protons traversing the tissues was estimated in which high conformity was obtained between our computation and the data taken from HZETRN model [13]. Furthermore, depth dose distribution as well as lateral broadening of absorbed dose at various depths in the tissues were computed. Most noteworthy, an outstanding consistency was obtained between our results and those

calculated by the GEANT4.5.2 [24] as well as the Monte Carlo simulations [25] for the Bragg peak position. In addition, for 160.7 MeV protons in water, depth dose distribution computed by the HPM compared with the experimental results of Paganetti [24] to highlight the precision of the homotopy perturbation method. Consequently, following the analysis of the results demonstrate that this method can be an applicable numerical technique with high accuracy in investigations related to hadrontherapy.

REFERENCES

1. G. Kraft, *Tumor Therapy with Heavy Charged Particles*, Prog. Part. Nucl. Phys., **45**, S473–S544 (2000).
2. M. Goitein, A.J. Lomax, E.S. Pedroni, *Treating cancer with protons*, Phys. Tod., **55**, 45–50 (2002).
3. Y. Hirao, H. Ogawa, S. Yamada, Y. Sato, T. Yamada, K. Sato, A. Itano, M. Kanazawa, K. Noda, K. Kawachi, M. Endo, T. Kanai, T. Kohno, M. Sudou, S. Minohara, A. Kitagawa, F. Soga, E. Takada, S. Watanabe, K. Endo, M. Kumada, S. Matsumoto, *Heavy ion synchrotron for medical use HIMAC project at NIRS-Japan*, Nucl. Phys. A, **538**, 541–550 (1992).
4. S. Braccini, *Scientific and Technological Development of Hadrontherapy*, http://arxiv.org/abs/1001.0860, 2010.
5. G.A.P. Cirrone, G. Cuttone, S.E. Mazzaglia, F. Romano, D. Sardina, C. Agodi, A. Attili, A.A. Blancato, M. Denapoli, F. Dirosa, P. Kaitaniemi, F. Marchetto, I. Petrovic, A. Ristic-Fira, J. Shin, N. Tarnavsky, S. Tropea, C. Zacharatou, *Hadrontherapy: a Geant4-Based Tool for Proton/Ion-Therapy Studies*, Prog. Nucl. Sci. Technol., **2**, 207–212 (2011).
6. M. Lee, A.E. Nahum, S. Webb, *An empirical method to build up a model of proton dose distribution for a radiotherapy treatment planning package*, Phys. Med. Biol., **38**, 989–998 (1993).
7. H. Szymanowski, U. Oelfke, *Two-dimensional pencil beam scaling: an improved proton dose algorithm for heterogeneous media*, Phys. Med. Biol. **47**, 3313–3330 (2002).
8. R. Fujimoto, T. Kurihara, Y. Nagamine, *GPU-based fast pencil beam algorithm for proton therapy*, Phys. Med. Biol., **56**, 1319–1328 (2011).
9. B. Schaffner, E. Pedroni, A. Lomax, *Dose calculation models for proton treatment planning using a dynamic beam delivery system: an attempt to include density heterogeneity effects in the analytical dose calculation*, Phys. Med. Biol., **44**, 27–41 (1999).
10. J.S. Li, B. Shahine, E. Fourkal, C.M Ma, *A particle track-repeating algorithm for proton beam dose calculation*, Phys. Med. Biol., **50**, 1001–1010 (2005).
11. P. Yepes, S. Randeniya, P.J. Taddei, W.D. Newhauser, *Monte Carlo fast dose calculator for proton radiotherapy: application to a voxelized geometry representing a patient with prostate cancer*, Phys. Med. Biol., **54**, *1*, N21–28 (2009).
12. M. Fippel, M. Soukup, *A Monte Carlo dose calculation algorithm for proton therapy*, Med. Phys., **31**, 2263–2273 (2004).
13. C.J. Mertens, J.W. Wilson, S.A. Walker, J. Tweed, *Coupling of multiple Coulomb scattering with energy loss and straggling in HZETRN*, Advances in Space Research, **40**, 1357–1367 (2007).
14. L.A. Bergman, B.F. Spencer, *On the numerical solution of the Fokker–Planck equation for nonlinear stochastic systems*, Nonlinear. Dyn., **4**, 357–372 (1993).
15. L.C. Shiau, T.Y. Wu, *A finite-element method for analysis of a nonlinear system under stochastic parametric and external excitation*, Int. J. Nonlinear. Mech., **31**, 193–203 (1996).
16. H. Noshad, S.S. Bahador, *Investigation on energy straggling of protons via Fokker-Planck equation*, Nucl. Instrum. Methods Phys. Res., Sect. B, **288**, 89–93 (2012).

17. J.J. Brey, J.M. Casado, M. Morillo, *Spectral density for a nonlinear Fokker-Planck model: Monte Carlo and analytical studies*, Phys. Rev. A, **32**, 2893–2898 (1985).
18. M. Soler, F.C. Martinez, J.M. Donoso, *Integral kinetic method for one dimension: the spherical case*, J. Stat. Phys., **69**, 813–835 (1992).
19. M. El-Shahed, *Application of He's homotopy perturbation method to Volterra's integro differential equation*, Int. J. Nonlinear Sci. Numer. Simul., **6**, *2*, 163–168 (2005).
20. S. Momani, S. Abuasad, *Application of He's variational iteration method to Helmholtz equation*, Chaos, Solitons & Fractals., **27**, 1119–1123 (2006).
21. E. Yusufoglu, *Variational iteration method for construction of some compact and noncompact structures of Klein-Gordon equations*, Int. J. Nonlinear Sci. Numer. Simul., **8**, *2*, 153–158 (2007).
22. D.D. Ganji, G.A. Afrouzi, R.A. Talarposhti, *Application of variational iteration method and Homotopy-perturbation method for nonlinear heat diffusion and heat transfer equations*, Phys. Lett. A, **368**, 450–457 (2007).
23. R. Yulita Molliq, M.S.M. Noorani, I. Hashim, *Variational iteration method for fractional heat- and wave-like equations*, Nonlinear Analysis: Real World Applications, **10**, 1854–1869 (2009).
24. A.J. Wroe, I. Cornelius, A. Rosenfeld, *The role of nonelastic reactions in absorbed dose distributions from therapeutic proton beams in different medium*, Med. Phys., **32**, *1*, 37–41 (2005).
25. H. Noshad, N. Givechi, *Proton therapy analysis using the Monte Carlo method*, Radiat. Meas., **39**, 521–524 (2005).
26. B. Rossi, *High Energy Particles*, Prentice-Hall, Inc., Englewood Cliffs, New Jersey, 1952, pp. 64–67.
27. L. Eyges, *Multiple scattering with energy loss*, Phys. Rev., **74**, 1534–1535 (1948).
28. J.H. He, *A coupling method of a homotopy technique and a perturbation technique for non-linear problems*, Int. J. Nonlinear. Mech. **35**, 37–43 (2000).
29. J.H. He, *Homotopy perturbation method for solving boundary value problems*, Phys. Lett. A, **350**, 87–88 (2006).
30. J.H. He, *Recent development of the homotopy perturbation method*, Topol. Method. Nonl. An., **31**, 205–209 (2008).